

Photoelectron Spectroscopy Studies of $\text{Ru}(\text{dcbpyH}_2)_2(\text{NCS})_2/\text{CuI}$ and $\text{Ru}(\text{dcbpyH}_2)_2(\text{NCS})_2/\text{CuSCN}$ Interfaces for Solar Cell Applications

Boriss Mahrov,^{†,‡} Gerrit Boschloo,[†] Anders Hagfeldt,[†] Hans Siegbahn,[‡] and Håkan Rensmo^{*,‡}

Department of Physical Chemistry, Uppsala University, Box 579, SE-751 23 Uppsala, Sweden, and
Department of Physics, Uppsala University, Box 530, SE-751 21 Uppsala, Sweden

Received: December 17, 2003; In Final Form: April 2, 2004

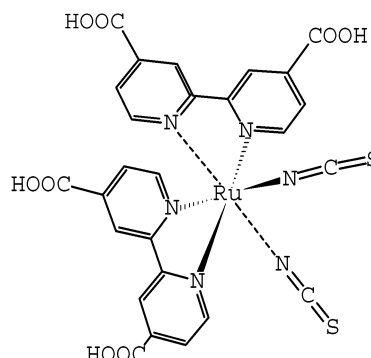
In this work, the electronic structure of the wide band gap hole conductors CuI and CuSCN in contact with an organic dye ($\text{Ru}(\text{dcbpyH}_2)_2(\text{NCS})_2$, *cis*-bis(4,4'-dicarboxy-2,2'-bipyridine)bis(isothiocyanato)ruthenium(II)) were investigated by means of photoelectron spectroscopy. The experiments show specific interaction between the NCS groups of the dye molecules and the CuI and CuSCN surfaces. For CuI there are strong indications that the dye molecules interact with CuI through both NCS ligands. Also, one of the carboxylic groups is affected by the surface adsorption on the CuI substrate. For the CuSCN surface the results indicate that about half of the molecules interact with the surface through both NCS ligands, that about half of the molecules interact with the surface through one NCS ligand, and that there is no specific interaction with the carboxylic groups. The measurements also reveal changes in the electronic structure of the dye molecule when adsorbed onto the substrates. In particular, changes in the upper valence electronic structure, important for the function of this material combination in a solar cell device, are discussed.

1. Introduction

Dye-sensitized nanostructured solar cells (DNSC) have become a promising alternative in the search for cost-effective and environment-friendly light to electrical energy converting systems.^{1–4} In such solar cells light absorbed by dye molecules (e.g., $\text{Ru}(\text{dcbpyH}_2)_2(\text{NCS})_2$, *cis*-bis(4,4'-dicarboxy-2,2'-bipyridine)bis(isothiocyanato)ruthenium(II), Chart 1) generates a photovoltaic output. In the most efficient DNSC the key process takes place at an interface between a dye-sensitized nanostructured semiconductor film and a liquid electrolyte. One advantage in combining the dye-sensitized nanostructured film and a liquid is that the liquid easily penetrates the nanonetwork, resulting in a huge interface active in the conversion process.

Encapsulation of the liquid electrolyte in these cells leads, however, to several technological problems such as solvent evaporation, degradation, and seal imperfection. These problems have encouraged studies in which the liquid redox electrolyte in dye-sensitized solar cells is replaced with solid-state equivalents, such as polymer–gel electrolytes,⁵ conducting organic polymers,⁶ ionic conductive polymer electrolytes,⁷ organic hole conductors,⁸ and inorganic semiconductors.⁹ CuI and CuSCN are p-type semiconductors that are suitable as hole conductors in dye-sensitized solar cells, and a number of attempts in the preparation of devices have been made.^{9–12} These materials are transparent, have good conductivity, and possess favorable valence band positions, which allow hole injection from oxidized or excited dye molecules. Furthermore they can be applied onto dye-sensitized TiO_2 electrodes using low-temperature methods. For solar cells based on TiO_2 sensitized with $\text{Ru}(\text{dcbpyH}_2)_2(\text{NCS})_2$ efficiencies on the order of 2% are achieved with CuSCN¹³ and up to 3.75% with CuI as the hole conductor.¹⁴

CHART 1: $\text{Ru}(\text{dcbpyH}_2)_2(\text{NCS})_2$



The photoconversion yields of these heterojunctions depend largely on the electron-transfer processes between the dye molecule and the semiconductor surface. This in turn is related to the geometrical and electronic structure of the dye in the heterojunction environment. Photoelectron spectroscopy (PES) is a route to the understanding of such properties and is particularly useful for surface analysis. In PES effects on the core level binding energy can be used to study element-specific interactions between the materials, while valence level measurements can be used to investigate energy matching and the changes in density of states in the frontier electronic structure. We have previously performed such studies on the dye/ TiO_2 interface.^{15–17} In the current study we focus on the specific dye adsorption from solution of $\text{Ru}(\text{dcbpyH}_2)_2(\text{NCS})_2$ at CuI and CuSCN substrates and on possible changes in the upper valence electronic structure (e.g., in the highest occupied molecular orbital, HOMO), when the dye interacts with the substrate.

2. Experimental Section

CuI and CuSCN sample preparation was similar to the procedure reported previously.^{9,10} The CuI and CuSCN films

* To whom correspondence should be addressed. E-mail: hakan.rensmo@fysik.uu.se.

[†] Department of Physical Chemistry.

[‡] Department of Physics.

were deposited by spraying a solution at 50 °C (CuI was dissolved in acetonitrile, CuSCN in *n*-propylsulfide, 1% by mass) onto conductive glass (50 °C) TEC-8 covered with a nanostructured TiO₂.¹⁸ The substrates were completely covered with hole conductor materials.

The CuSCN and CuI films were soaked in ethanol (Kemetyl, 99.6%) and dye solutions of Ru(dcbpyH₂)₂(NCS)₂ in ethanol. For the dye sensitization of the CuSCN substrate a 0.5 mM dye solution was used, while a 0.05 mM dye solution was used for the CuI substrate. If not stated otherwise, dye-sensitization time was 10 min. All dye-sensitized hole conductor films were rinsed by dipping them into ethanol. The procedures reported here yield close to monolayer coverage (see below). However, when dye-sensitizing CuI in higher dye concentrations or for longer times, the signal from the substrate vanishes, which shows that the dye coverage is higher and that some kind of multilayer is formed.¹⁵

For the preparation of films containing dye molecules that are not specifically bonded to a substrate, we used as a substrate layers of TiO₂ (thickness about 200 nm) on TEC-8 conducting glass. The TiO₂ was made by spray pyrolysis deposition at 450 °C. The spray solution used was titanium(IV) isopropoxide (2.4 mL) and acetyl acetone (3.6 mL) in ethanol (54 mL).¹⁹ These substrates were soaked for 30 min in 0.5 mM dye solutions of Ru(dcbpyH₂)₂(NCS)₂ in ethanol, but they were not rinsed. This preparation gave a multilayer coverage of the dye with only minor effects from the substrate itself and is hereafter referred to as nonbonded dye molecules.

The photoelectron spectroscopy (PES) measurements were performed using synchrotron light at BL I411 at the Swedish National Laboratory MAX in Lund.²⁰ The takeoff angle (θ) used was 70°, and the angle between photon polarization and photoelectron direction was 0°. If not stated otherwise, the spectra for the dye-sensitized CuI and CuSCN are energy-calibrated and intensity-normalized with respect to the N 1s peak originating from the bipyridine as measured for the nonbonded dye molecule. Energy-referencing of the nonbonded dye molecule was made with respect to the main C 1s peak, which was set to 285.0 eV. The overall resolution of the Cu 2p and I 3d spectra was better than 1.0 eV. For all other spectra the overall resolution was better than 0.4 eV. Repeated scans on the same spot illuminated for different times were recorded in order to follow a possible radiation damage process. No changes in peak shapes were detected, showing that no such damage process occurred within the time scale of the measurement.

3. Results and Discussion

3.1. Structure of the Ru(dcbpyH₂)₂(NCS)₂/CuI Interface.

3.1.1. Uncoated CuI. The photoelectron core level spectra of CuI are dominated by strong Cu 2p and I 3d peaks shown in Figure 1. Samples prepared by solution-based methods also display traces of oxygen and carbon in the surface region, which is expected for ex-situ-prepared samples. However, due to the presence of a single Cu 2p_{3/2} peak and after comparing the relative intensities (O 1s vs I 3d) for the as-prepared CuI film with those obtained for sensitized films (see below), the contributions from contaminants are found to be less important. In the O 1s spectra for the dye-sensitized CuI films the contributions are estimated to be less than 5%.

Before sensitizing the samples, using ethanol-based dye solutions, possible surface reactions due to the solvent were checked for. Dipping the samples into ethanol has very little effect on the Cu 2p and I 3d core level spectra.

3.1.2. Dye Sensitization of CuI: Cu 2p and I 3d Core Levels.

The surface structure for the dye adsorbed at the CuI surface

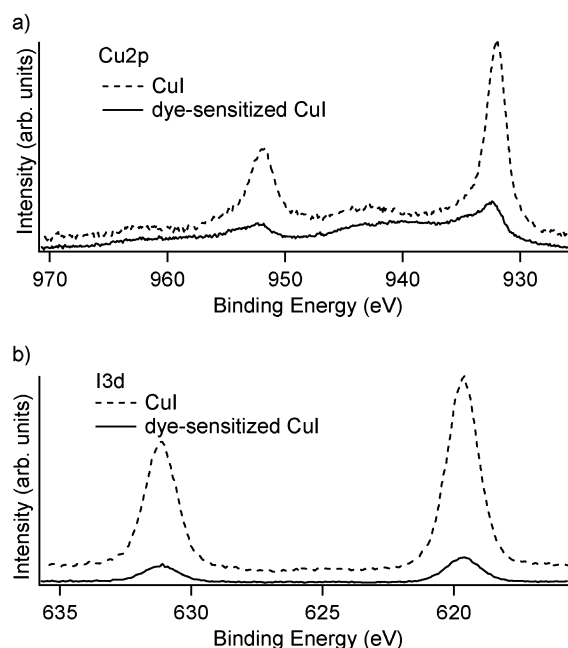


Figure 1. (a) Cu 2p core level spectra of uncoated and dye-sensitized CuI surfaces. (b) I 3d core level spectra of uncoated and dye-sensitized CuI surfaces. (The intensity is normalized versus the photon flux, and the uncoated spectra are energy-calibrated vs the I 3d peak; $h\nu = 1200$ eV).

was studied, and effects of the sensitization are clearly seen in all core level spectra. In particular, both the Cu 2p and I 3d are damped after 10 min of dye sensitization; see Figure 1. Dye-sensitizing the samples for a longer time or at higher concentrations further increases the damping, i.e., increases the amounts of dye at the surface, forming a multilayer. In a previous investigation on ZnO such multilayer formation was explained by aggregation with ions dissolved from the substrate (Zn²⁺/dye aggregates).¹⁵

From the damping some estimates of the surface coverage can be obtained using the expression $I = I_0 \exp[-d/(\lambda \sin \theta)]$ and assuming a mean free path, λ , of about 1 nm.²¹ Using the ratio of the substrate peak (Cu 2p or I 3d) measured before and after the sensitization (I/I_0), Figure 1, a layer thickness, d , of about 1–2 nm is calculated. Although this procedure contains uncertainties, in particular with respect to the mean free path for this Ru complex, the value is fairly close to the diameter of the molecule (about 1 nm) and indicates that the amount adsorbed is close to a monolayer. Thus, although some multilayer effects, such as substrate-induced dye aggregation,¹⁵ cannot be excluded, effects from interaction between the dye molecule and the interface largely influence the spectra reported below.

A closer look at the Cu 2p spectrum shows that parts of the Cu atoms are strongly affected by the dye adsorption. A new shoulder is observed at lower binding energies after the sensitization. The position of this shoulder is shifted about +2.5 eV in accordance with what one would expect when oxygen binds to Cu.²² This suggestion is further supported by the O 1s spectra reported below.

Contrary to what is observed in the Cu 2p region, no new features are observed in the I 3d spectrum, Figure 1b.

3.1.3. Dye Sensitization of CuI: O 1s, N 1s, C 1s, Ru 3d, and S 2p Core Levels. Further information on the interaction between the dye molecule and the substrate can be obtained by comparing the dye core level spectra for the dye-sensitized CuI surface with that of nonbonded dye molecules. The O 1s spectrum for

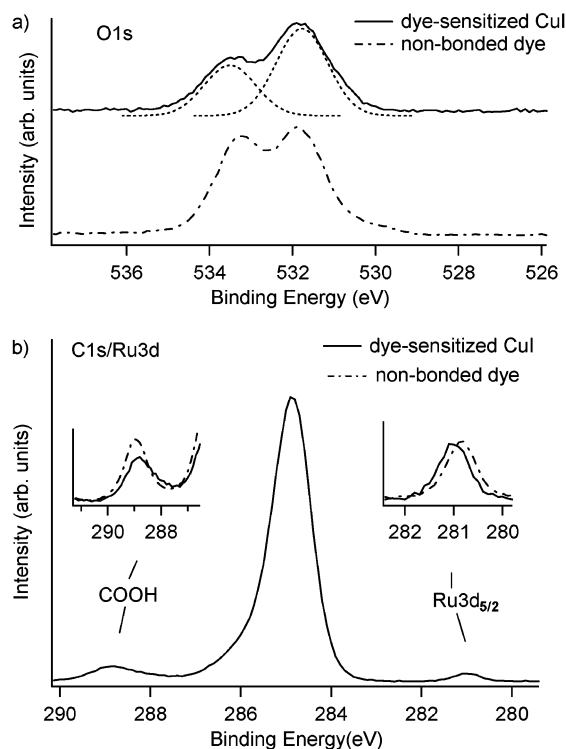


Figure 2. (a) O 1s core level spectra of nonbonded dye molecules and dye-sensitized CuI surface ($h\nu = 758$ eV). From the curve fit, dotted line, the intensity relation between the two peaks for the dye-sensitized CuI is estimated to be 3:5. (b) C 1s/Ru 3d core level spectra of nonbonded dye molecules and dye-sensitized CuI surface ($h\nu = 454$ eV).

the nonbonded molecule, Figure 2a, contains two peaks with the same intensity, corresponding to the two nonequivalent oxygen atoms in the carboxyl groups. The higher binding energy peak represents the protonated oxygen atoms, while the lower binding energy peak represents the doubly bonded oxygen atoms.¹⁵ The spectrum measured for the dye-sensitized CuI also contains at least two peaks in the O 1s region. In this case, however, the intensity has moved from the binding energy region of the protonated oxygen toward the lower binding energies. This shift suggests some interaction with the substrate material, probably via the Cu atoms as discussed above. The intensity relation between the peaks for the dye-sensitized CuI is about 3:5, indicating that one of the carboxylic groups has been deprotonated upon surface adsorption (see the curve fit in Figure 2a, dotted line).

Also in the C 1s spectrum, see Figure 2b, features are observed, supporting this picture. The peak at 289 eV originates from the carboxylic carbon, and the structure of this peak for a nonbonded molecule is compared with the structure measured for the dye-sensitized CuI; see the inset in Figure 2b. This peak is broadened toward lower binding energies upon surface adsorption. This effect is also observed when the dye binds to oxide surfaces.¹⁶

Possible interactions between the NCS group and the substrate can be investigated by measuring the N 1s and S 2p core level spectra. The N 1s core level spectra for the dye-sensitized CuI surface and for the nonbonded dye molecules are shown in Figure 3a. In the spectrum of the nonbonded dye molecules two clearly resolved peaks are observed representing the bipyridine nitrogen (the peak at higher binding energy) and the NCS nitrogen (the peak at lower binding energy). The structure of the N 1s spectrum measured for the dye-sensitized CuI surface is similar except for a clear shift of the peak originating from

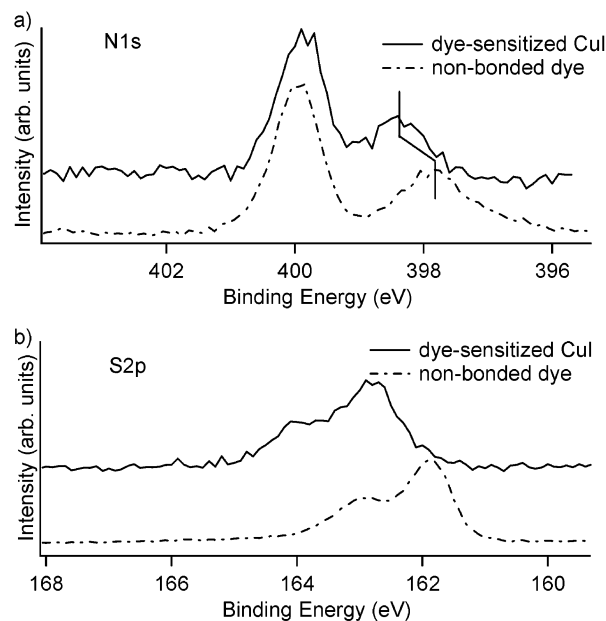


Figure 3. (a) N 1s core level spectra of nonbonded dye molecules and a dye-sensitized CuI surface ($h\nu = 454$ eV). (b) S 2p core level spectra of nonbonded dye molecules and a dye-sensitized CuI surface ($h\nu = 454$ eV).

NCS. This peak shifts about +0.6 eV, showing a strong interaction between the NCS groups with the surface. Since no clear feature is observed at about 397.9 eV, this result also indicates that both of the NCS groups are affected and probably bind to the CuI surface. This conclusion is further supported by the S 2p spectra in Figure 3b. A shift of +0.9 eV is obtained for the position of the S 2p signal for the nonbonded dye molecules compared with that obtained from the dye-sensitized CuI.

Comparing the results reported here, obtained for samples prepared using solution-based methods, with those from samples prepared by evaporation of CuI onto a dye-sensitized TiO₂ (dye/TiO₂) surface in situ,²³ the general picture is rather similar; i.e., CuI specifically interacts with the NCS ligand of the dye molecule. Some differences are, however, observed. In the present investigation both NCS groups seem to bind to the CuI substrate, which is not the case when CuI is evaporated onto the dye/TiO₂ surface. This difference indicates that the interactions with two materials in a true heterojunction environment (TiO₂/dye/CuI) constrain the structure. Here, we also observe evidence for a specific interaction involving the Cu atoms in the substrate and carboxylic groups in the dye contrary to what was obtained in the in-situ preparation.²³ The reason for this discrepancy is presently unclear but might reflect the influence of a liquid environment.

The shifts in the core levels indicate substantial charge redistribution in the dye molecule upon adsorption. In this context we note that also the Ru 3d_{5/2} shifts +0.2 eV when binding to the surface. Charge redistributions in the dye molecule are expected to have important consequences also for the frontier electronic structure, in particular on the upper valence structure.²⁴ Such effects are discussed further below.

3.2. Structure of the Ru(dcbpyH₂)₂(NCS)₂/CuSCN Interface. **3.2.1. Uncoated CuSCN.** The PES core level spectra of the CuSCN substrate are shown in Figure 4. The Cu 2p and S 2p spectra show a single spin-orbit split doublet, and the N 1s (Figure 4b) spectrum shows a single peak. As mentioned above, samples prepared by solution-based methods may display traces of oxygen and carbon at the surface, which is expected for ex-

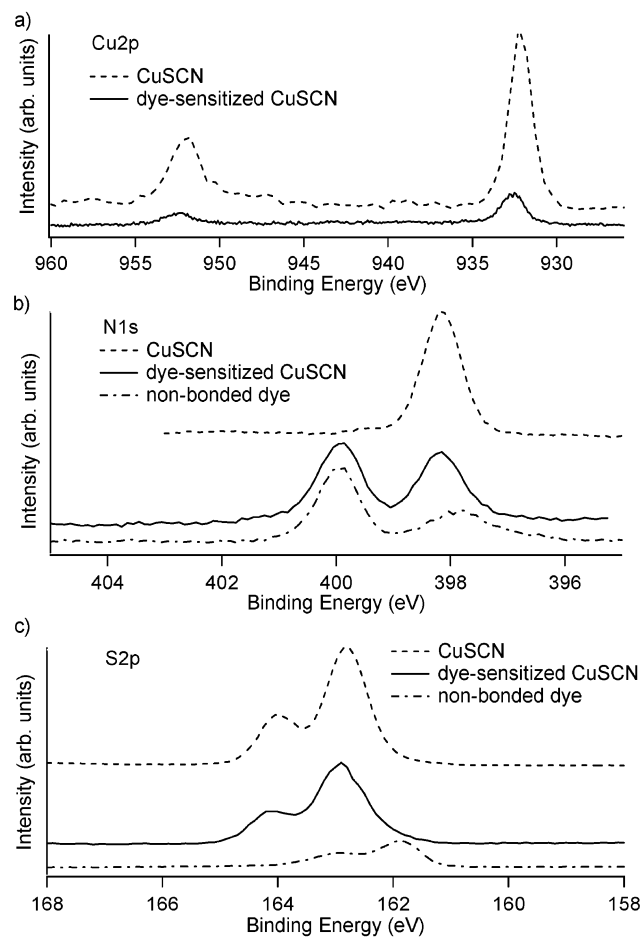


Figure 4. (a) Cu 2p core levels spectra of the uncoated CuSCN surface and the dye-sensitized CuSCN surface ($h\nu = 1200$ eV). The intensity is normalized vs the photon flux. (b) N 1s core level spectra of the uncoated CuSCN (top, $h\nu = 758$ eV). The N 1s core levels spectra of the nonbonded dye molecules and the dye-sensitized CuSCN surface (bottom, $h\nu = 454$ eV). (c) S 2p core level spectra of the nonbonded dye molecules, the uncoated CuSCN surface, and the dye-sensitized CuSCN surface ($h\nu = 454$ eV). The binding energy scales for the uncoated CuSCN were fixed using the S 2p_{3/2} peak maxima in the dye-sensitized sample.

situ-prepared samples. Comparing the two substrates studied here, such contributions of oxygen were found to be much less in the case of CuSCN. Also for CuSCN, possible surface reactions due to the solvent were checked for. Dipping the samples into ethanol was found to have very little effect on the core level structure.

3.2.2. Dye Sensitization of CuSCN: Cu 2p, O 1s, and C 1s Spectra. Dye sensitization of CuSCN results in adsorption of the dye at the substrate surface. Contrary to dye sensitization of CuI, no effects of multilayer formation or aggregation of the dye could be detected even after long sensitization times and at higher dye concentrations. The decrease in substrate intensity was in accordance with that expected for a coverage of about one monolayer, Figure 4a. In the case of CuSCN, dye sensitization did not result in any new features in the Cu 2p core level peaks.

The comparison of the O 1s and the carboxylic C 1s core level spectra of the dye-sensitized CuSCN and the nonbonded dye molecules give information about possible interactions between the carboxylic groups and the CuSCN substrate. As seen from Figure 5a, the ratio between the two different O 1s peaks remains unchanged (1:1) upon surface adsorption and the two spectra are very similar. Also, the peaks from the carbons

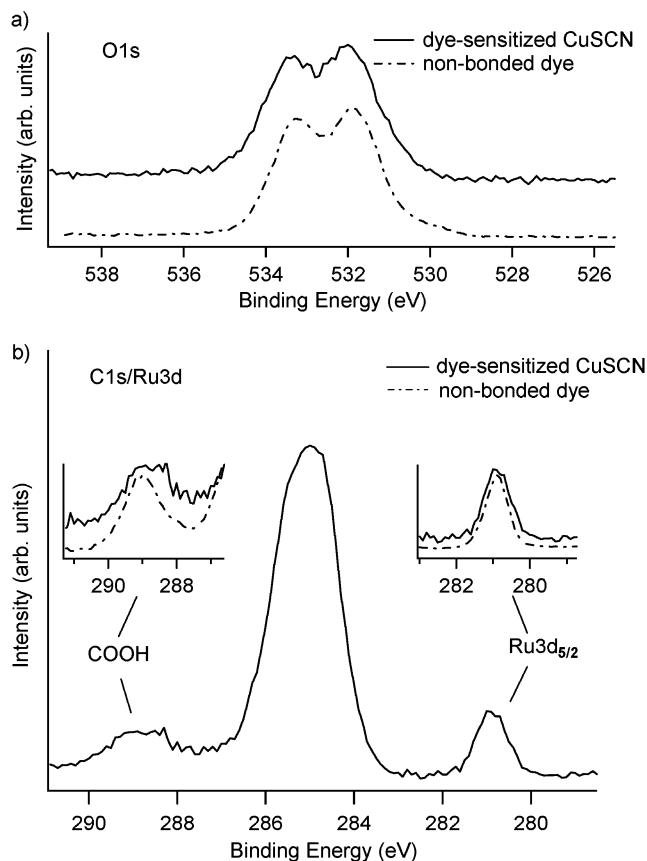


Figure 5. (a) The O 1s core level spectra of nonbonded dye molecule and dye-sensitized CuSCN surface ($h\nu = 758$ eV). (b) C 1s/Ru 3d core level spectra of nonbonded dye molecule and dye-sensitized CuSCN surface ($h\nu = 758$ eV).

in the carboxylic groups, seen in the C 1s spectra, Figure 5b, show no changes in position when comparing the nonbonded and the bonded dye molecules. From the similarity in the Cu 2p, O 1s, and C 1s spectra for a bonded and a nonbonded molecule, it is concluded that the dye does not bind to the CuSCN surface via the carboxyl groups.

3.2.3. Dye Sensitization of CuSCN: N 1s and S 2p Spectra. The nitrogen and sulfur core level spectra provide information about the specific adsorption of the dye molecules onto the CuSCN surface. The N 1s spectrum measured for the dye-sensitized CuSCN contains two features of similar intensity and is clearly different from that of the nonbonded dye molecules; see Figure 4b. Based on a comparison of the spectrum for the dye-sensitized CuSCN with the N 1s spectrum of nonbonded dye molecules and the N 1s spectrum of the substrate itself, the feature at lower binding energy can be associated with a mixture of the nitrogens in the NCS ligand in the molecules and in the CuSCN substrate. Similarly, the S 2p spectra contain contributions from both sulfur originating from the substrate and sulfur originating from the dye molecule, Figure 4c. A detailed analysis of the N 1s and the S 2p spectra is described below.

Deconvolutions of the N 1s and S 2p were performed assuming three types of NCS groups: NCS in the CuSCN substrate, NCS in the dye not specifically linked to the substrate, and NCS in the dye specifically linked to the substrate. Based on measurements from the CuSCN substrate and the nonbonded dye molecules, the following constraints were used: (a) The peak shape, relative binding energy, and relative intensity of nitrogen and sulfur in NCS originating from the substrates were taken from the measurements of the uncoated CuSCN film. The

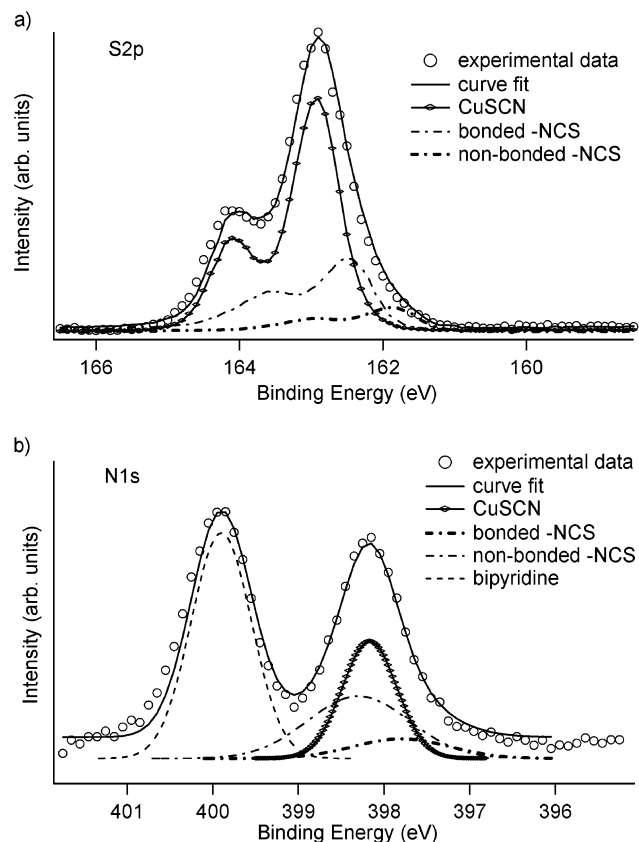


Figure 6. Deconvolution of (a) S 2p and (b) N 1s spectra originating from dye-sensitized CuSCN surface ($h\nu = 454$ eV). See text for details.

absolute binding energy positions for these substrate peaks were fixed using the S 2p_{3/2} peak maxima in the dye-sensitized sample. (b) The peak shape, relative binding energy, and relative intensity of nitrogen and sulfur in NCS originating from the dye not specifically interacting with the CuSCN substrate were taken from measurements of the nonbonded dye molecule (the dye multilayer). The absolute binding energy positions in this case were fixed using the bipyridine nitrogens. (c) The shape and relative intensity of N 1s and S 2p originating from the dye NCS ligand and which specifically adsorbs to the CuSCN substrate were taken from measurements of the nonbonded dye molecule. Summarizing the deconvolution procedure, the only variables were the relative intensities of the three contributing NCS groups and the positions of the N 1s and S 2p originating from the dye NCS ligands specifically linked to the surface.

After evaluating the experimental data according to the above constraints, one may conclude that all three contributions are needed in order to fit the data; i.e., some NCS ligands specifically link to the CuSCN substrate, but there are also contributions from NCS ligands not specifically linked to the substrate. In an attempt to quantify the results, we obtain a reasonable fit, see Figure 6, when about 75% of the NCS ligands shifts in energy position and the rest remain nonbonded. These results indicate that about half of the dye molecules are linked through both NCS ligands and the other half through only one ligand. The deconvolution in Figure 6 indicates that the position of the S 2p level is shifted from the original position by about +0.6 eV toward higher binding energy, while the N 1s level is shifted with about +0.4 eV. Although the quantitative results from a deconvolution procedure, as described above, always contain some uncertainties, we note that the obtained shifts are similar to those measured for the dye absorbed on CuI although the magnitude is somewhat smaller. Again we note that charge

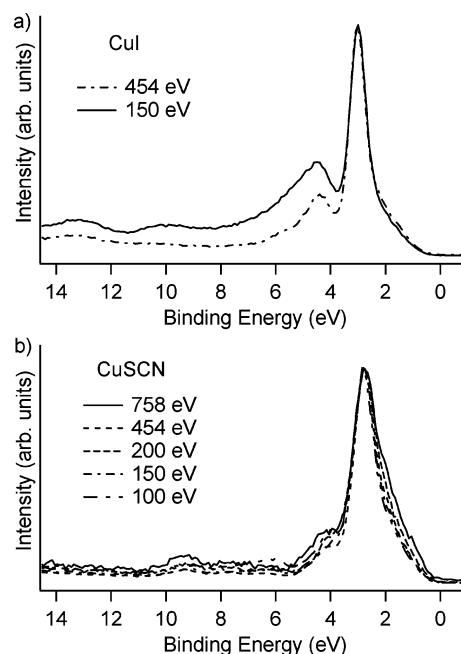


Figure 7. (a) Valence band spectra of the uncoated CuI surface measured at two photon energies (energy-calibrated and intensity-normalized vs the Cu 3d peak at 3.0 eV). (b) Valence band spectra of the uncoated CuSCN surface measured at different photon energies (energy-calibrated and intensity-normalized vs the Cu 3d peak at 2.9 eV).

redistribution within the dye molecule should have effects also on the frontier electronic structure, although, in the case of dye-sensitized CuSCN, we do not observe clear effects on the Ru 3d_{5/2} core level.

In summary there is clear evidence for chemical bond formation between the CuSCN surface and the NCS ligands of the dye, while no interaction with the carboxylic group is observed.

3.3. Valence Electronic Structure of the Dye-Sensitized CuI and CuSCN Interface. The CuI valence spectra measured at two different photon energies are shown in Figure 7a. The valence structure for CuI reported in this study is similar to that obtained earlier using Al K α .²⁵ The spectra contain three main features: a smaller peak at about 4.5 eV, a larger peak at about 3 eV, and a shoulder at lower binding energies (0.5–1.5 eV). As indicated by the photon energy dependence, these regions have different orbital character and were earlier referred to as mainly I 5p character (4.5 eV), Cu 3d character (3 eV), and Cu 3d/I 5p hybridization character (0.5–1.5 eV).²⁶

The valence spectrum of CuSCN also contains three main features, and the valence structure is similar to that of the copper halides, Figure 7b. However, in a more detailed comparison between the CuI and the CuSCN spectra, we observe that the width of the main peak is slightly broader and the shoulder at lower energies is more pronounced in the spectrum of CuSCN. As for CuI, the valence spectrum of CuSCN shows a photon energy dependence in which the lower energy levels are more intense at higher photon energies, indicating that the regions have different orbital characters. On the basis of the similarity to the CuI valence spectra, we attribute the main peak as mainly having a Cu 3d character, while the shoulder at lower energies is a combination of Cu 3d and the p orbitals from the NCS group. The comparison between the two materials indicates that although their overall structure is similar, the upper valence electronic structure is influenced by the anion.

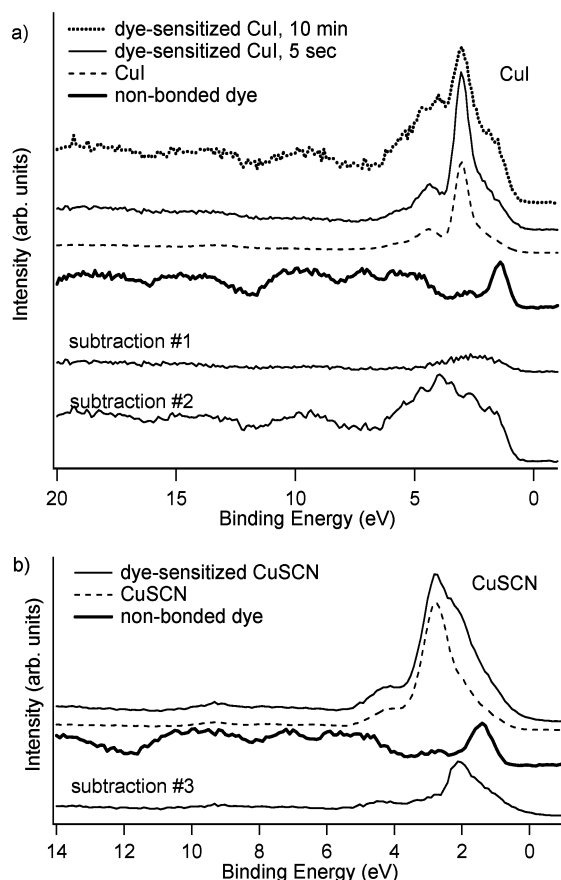


Figure 8. (a) Valence band spectra of the nonbonded dye molecules, the uncoated CuI surface, and the CuI surfaces dye-sensitized for 5 s and 10 min (the spectra of uncoated CuI have been energy-calibrated vs the Cu 3d peak at 3.0 eV). Subtraction of the uncoated CuI spectrum from the 5 s dye-sensitized CuI spectrum (subtraction no. 1) or from the 10 min dye-sensitized CuI spectrum (subtraction no. 2) are shown at the bottom. (b) Valence band spectra of the nonbonded dye molecules, the uncoated CuSCN surface, and the dye-sensitized CuSCN surface. Subtraction of the uncoated CuSCN spectrum from the dye-sensitized CuSCN spectrum (subtraction no. 3) is shown at the bottom (the spectra of uncoated CuSCN have been energy-calibrated vs the Cu 3d peak at 2.9 eV).

To shed some light on the specific interactions between the dye and the substrate and how these interactions influence energy matching and the frontier electron structure, we compare the valence spectra for sensitized CuI with that of the nonbonded molecule. In Figure 8a the valence spectra for the nonbonded dye molecules and the uncoated CuI substrate are shown together with the spectra for CuI dye-sensitized for 5 s and 10 min. The larger sensitizing time represents a film with about one monolayer coverage, while the short sensitizing time represents a film with submonolayer coverage. (This was determined from the damping in the substrate signal; see the discussion above.) Comparing these spectra, it is noticed that the valence structure is clearly affected by the dye sensitization. Specifically, the structure at higher (4 eV) and lower (1–2 eV) energy increases with respect to the main peak (at about 2.5 eV) upon dye sensitization. The increase at lower energy indicates an overlap between the HOMO energy level of the dye and the valence band of the hole conductor, a result expected from the comparison with the spectrum of the nonbonded dye molecule. This result is in line with the function of this particular material combination in energy conversion applications.⁹

As expected the effect on the valence spectrum from the dye molecule is larger when increasing the amount of dye molecules

at the surface. For the CuI film with the higher dye coverage (10 min dye sensitization), we observe that the structure in the binding energy region 7–20 eV is rather similar to that of the nonbonded molecule. At lower binding energies, structures related to the substrate are still observed. In particular the structure referred to as Cu 3d in CuI is clearly distinguishable in both spectra.

As mentioned earlier, the dye upper valence electronic states should be largely affected by interactions with the NCS and, in turn, the Ru metal center. Redistribution of the upper valence structure is clearly seen when comparing the different PES valence spectra. We note that it was impossible to reproduce the valence spectra of the dye by a simple subtraction of the uncoated CuI spectrum from the 10 min dye-sensitized CuI spectrum or from the 5 s dye-sensitized CuI spectrum; see Figure 8a. Although subtractions such as those shown in Figure 8a should not be overinterpreted, this result indicates that the upper valence structure is largely affected by the dye sensitization.

A similar discussion can also be applied for the dye-sensitized CuSCN (see Figure 8b); i.e., the frontier electronic structure changes when adsorbing at the CuSCN. In particular we note the growth of states at lower binding energy (below the HOMO measured for the nonbonded dye molecule). Such changes are important for the function of this particular material combination. It is, for example, expected to change the absorption properties although it is noted that the maximum in the photocurrent action spectra for a TiO₂/Ru dye/CuI or TiO₂/Ru dye/CuSCN DNSC is rather similar to the absorption maximum in the visible region when the dye is dissolved in ethanol solution.^{10,18,27}

4. Conclusion

Photoelectron spectroscopic measurements have been made on a series of uncoated and dye-sensitized (Ru(dcbpyH₂)₂-(NCS)₂) CuI and CuSCN surfaces. For the CuI, the measurements indicate bond formation with both NCS ligands to the surface. The measurements on dye-sensitized CuI also indicate specific interaction with one of the carboxylic groups. For the CuSCN, the measurements indicate bond formation with the dye NCS ligands to the surface but no interaction was observed with the carboxylic groups. The analysis on the dye-sensitized CuSCN indicates that about half of the dye molecules bind to the surface via one NCS ligand and the rest via both ligands. The specific interactions also lead to changes in the valence electronic structure of the dye. Together the results reported here indicate that the direct link between the substrate and the dye molecule have a large effect on the dye electronic structure. Such changes are of importance for the detailed understanding of the material matching and function of the DNSC, although the effects on, for example, light absorption properties or the final photoconversion efficiencies are difficult to estimate.

To further understand the interactions within a true DNSC heterojunction in detail, we recently performed complementary work on a complete TiO₂/Ru dye/CuI solid-state model system.²³ In this case CuI was deposited in situ onto a dye-sensitized TiO₂ surface and the formation of the dye/CuI interface and the changes brought upon the dye/TiO₂ interface could be monitored in a stepwise fashion. Also in this case a direct interaction between the dye NCS groups and the CuI is evident in the core level photoelectron spectra. However, probably due to the geometrical constraints imposed by the binding to the TiO₂ surface the fraction of NCS groups bonded to CuI was smaller.²³

Acknowledgment. The work has been carried out with financial support from the European Commission RTN-Project

HRNP-CT-2000-00141, the Swedish Science Foundation (VR), the Swedish Foundation for Strategic Research (SSF), the Swedish National Energy Administration, and the Göran Gustafsson Foundation.

References and Notes

- (1) O'Regan, B.; Grätzel, M. *Nature* **1991**, *353*, 737–740.
- (2) Hagfeldt, A.; Grätzel, M. *Chem. Rev.* **1995**, *95*, 94.
- (3) Grätzel, M. *Prog. Photovolt. Res. Appl.* **2000**, *8*, 171–185.
- (4) Grätzel, M. *Nature* **2001**, *414*, 338–344.
- (5) Yanagida, S.; Kambe, S.; Kubo, W.; Murakoshi, K.; Wada, Y.; Kitamura, T. *Z. Phys. Chem. Part I* **1999**, *212*, 31–38.
- (6) Murakoshi, K.; Kogure, R.; Wada, Y.; Yanagida, S. *Sol. Energy Mater. Sol. Cells* **1998**, *55*, 113.
- (7) Matsumoto, M.; Miyazaki, H.; Matsuhira, K.; Kumashiro, Y.; Takaoka, Y. *Solid State Ionics* **1996**, *89*, 263.
- (8) Bach, U.; Lupo, D.; Comte, P.; Moser, J. E.; Weissörtel, F.; Salbeck, J.; Spreitzer, H.; Grätzel, M. *Nature* **1998**, *395* (6702), 583–585.
- (9) Tennakone, K.; Kumara, G. R. R. A.; Kottegoda, I. R. M.; Wijayantha, K. G. U.; Perera, V. P. S. *J. Phys. D: Appl. Phys.* **1998**, *31*, 1492–1496.
- (10) Kumara, G. R. R. A.; Konno, A.; Senadeera, G. K. R.; Jayaweera, P. V. V.; De Silva, D. B. R. A.; Tennakone, K. *Sol. Energy Mater. Sol. Cells* **2001**, *69*, 195–199.
- (11) Tennakone, K.; Kumara, G. R. R. A.; Kumarasinghe, A. R.; Wijayantha, K. G. U.; Sirimanne, P. M. *Semicond. Sci. Technol.* **1995**, *10*, 1689–1693.
- (12) O'Regan, B.; Schwartz, D. T.; Zakeeruddin, S. M.; Grätzel, M. *Adv. Mater.* **2000**, *12*, 17.
- (13) O'Regan, B.; Lenzmann, F.; Muis, R.; Wienke, J. *Chem. Mater.* **2002**, *14*, 5023.
- (14) Kumara, G. R. A.; Kaneko, S.; Okuya, M.; Tennakone, K. *Langmuir* **2002**, *18*, 10493–10495.
- (15) Westermark, K.; Rensmo, H.; Siegbahn, H.; Keis, K.; Hagfeldt, A.; Ojamäe, L.; Persson, P. *J. Phys. Chem. B* **2002**, *106*, 10102–10107.
- (16) Rensmo, H.; Westermark, K.; Södergren, S.; Kohle, O.; Persson, P.; Lunell, S.; Siegbahn, H. *J. Chem. Phys.* **1999**, *111*, 2744–50.
- (17) Patthey, L.; Rensmo, H.; Persson, P.; Westermark, K.; Vayssieres, L.; Stashans, A.; Petersson, A.; Brühwiler, P. A.; Siegbahn, H.; Lunell, S.; Mårtensson, N. *J. Chem. Phys.* **1999**, *110* (12), 5913–5918.
- (18) Nazeeruddin, M. K.; Kay, A.; Rodicio, I.; Humphry-Baker, R.; Müller, E.; Liska, P.; Vlachopoulos, N.; Grätzel, M. *J. Am. Chem. Soc.* **1993**, *115*, 6382–90.
- (19) Kavan, L.; Grätzel, M. *Electrochim. Acta* **1995**, *40*, 643–652.
- (20) Svensson, S.; Forsell, J.-O.; Siegbahn, H.; Ausmees, A.; Bray, G.; Södergren, S.; Sundin, S.; Osborne, S. J.; Aksela, S.; Nömmiste, E.; Jauhiainen, J.; Jurvansuu, M.; Karvonen, J.; Barta, P.; Salaneck, W. R.; Evaldsson, A.; Lögdahl, M.; Fahlman A. *Rev. Sci. Instrum.* **1996**, *67*, 2149.
- (21) Hüfner, S. *Photoelectron Spectroscopy*, 3rd ed.; Springer-Verlag: Berlin Heidelberg, 2003.
- (22) Kawatsura, K.; Takeshima, N.; Imaoku, T.; Takahiro, K.; Mokuno, Y.; Horino, Y.; Sekioka, T.; Terasawa, M. *Nucl. Instr. and Methods B* **2002**, *193*, 877–882.
- (23) Karlsson, P. G.; Bolik, S.; Richter, J. H.; Mahrov, B.; Johansson, E.; Blomquist, J.; Uvdal, P.; Rensmo, H.; Siegbahn, H.; Sandell, A. *J. Chem. Phys.* accepted.
- (24) Rensmo, H.; Lunell, S.; Siegbahn, H. *J. Photochem. Photobiol. A: Chemistry* **1998**, *114*, 117–124.
- (25) Kono, S.; Ishii, T.; Sagawa, T.; Kobayashi, T. *Phys. Rev. Lett.* **1972**, *28*, 1385.
- (26) Ferhat, M.; Zaoui, A.; Certier, M.; Dufour, J. P.; Khelifa, B. *Mater. Sci. Eng. B* **1996**, *39*, 95.
- (27) Kumara, G. R. A.; Konno, A.; Shiratsuchi, K.; Tsukahara, J.; Tennakone, K. *Chem. Mater.* **2002**, *14*, 954.